VU VRIJE UNIVERSITEIT AMSTERDAM

VU Research Portal

Integrating geophysical, hydrochemical and hydrologic data to understand the freshwater resources on Nantucket Island, Massachusetts.

Marksammer, A.J.; Person, M.A.; Day-Lewis, F.D.; jr Lane, J.W.; Cohen, D.; Dugan, B.; Kooi, H.; Willett, M.

published in
Geophysical Monograph Series
2007

DOI (link to publisher)
10.1029/171GM12

document version
Publisher's PDF, also known as Version of record

Link to publication in VU Research Portal

citation for published version (APA)
Marksammer, A. J., Person, M. A., Day-Lewis, F. D., jr Lane, J. W., Cohen, D., Dugan, B., Kooi, H., & Willett, M. (2007). Integrating geophysical, hydrochemical and hydrologic data to understand the freshwater resources on Nantucket Island, Massachusetts. *Geophysical Monograph Series*. https://doi.org/10.1029/171GM12

General rights
Copyright and moral rights for the publications made accessible in the public portal are retained by the authors and/or other copyright owners and it is a condition of accessing publications that users recognise and abide by the legal requirements associated with these rights.

- Users may download and print one copy of any publication from the public portal for the purpose of private study or research.
- You may not further distribute the material or use it for any profit-making activity or commercial gain
- You may freely distribute the URL identifying the publication in the public portal ?

Take down policy
If you believe that this document breaches copyright please contact us providing details, and we will remove access to the work immediately and investigate your claim.

E-mail address:
vuresearchportal.ub@vu.nl

Download date: 04. May. 2023

Integrating Geophysical, Hydrochemical, and Hydrologic Data to Understand the Freshwater Resources on Nantucket Island, Massachusetts

Andee Jean Marksamer

Submitted to the faculty of the University Graduate School
in partial fulfillment of the requirements
for the degree
Master of Science
in the Department of Geological Sciences,
Indiana University
May 2007

Acknowledgements

I would like to thank my committee members, Dr. Mark Person, Dr. Gary Pavlis and Dr. Arndt Schimmelmann for their thorough review and helpful suggestions for this manuscript. I would like to mention a special appreciation to Dr. Mark Person, my faculty advisor, for his continued encouragement and support during my time at Indiana University. The knowledge I've gained in both hydrogeology and in basic scientific principles from Dr. Person will be forever remembered and appreciated as I advance through my professional career. In addition to the individuals above, I would also like to thank Dr. John Lane, Dr. Frederick Day-Lewis, Dr. Denis Cohen, Dr. Brandon Dugan, and Dr. Henk Kooi for their contributions to help get my thesis published.

I must also give a big thanks to my fellow labmates in the GeoFluids Computational Laboratory for always keeping me smiling even during the long days and late nights in the lab. It is also necessary to recognize Ken Dehart for his help at fixing all the computer problems that I incurred during my time at Indiana University. I would also like to thank the Wannacomet Water Company and Sarah Oktay and Tony Molis of the University of Massachusetts Boston Field Station for their logistical field support. Finally, I would like to thank my family and friends, but especially my husband, Ken Downey, for his continued love and support in all aspects of my life.

This research was supported by a grant from the National Science Foundation (EAR-0337634) to Mark Person. USGS contributions to this work were funded in part by the USGS Groundwater Resources Program.

Preface

This thesis is a draft of a manuscript that was recently submitted to the American Geophysical Union (AGU) for publication in an AGU Geophysical Monograph Series entitled, *Data Integration in Subsurface Hydrology*, edited by, David W. Hyndman, Frederick D. Day-Lewis, and Kamini Singha. The manuscript was submitted under the same title as this thesis. This monograph will be in publication Spring 2007. Co-authors for the published manuscript include Mark Person of Indiana University, Bloomington, IN, Frederick D. Day-Lewis and John Lane Jr. of the United States Geological Survey in Storrs, CT, Denis Cohen from Iowa State University, Ames, Iowa, Brandon Dugan from Rice University, Houston, TX, Henk Kooi from Vrije Universiteit, Amsterdam, The Netherlands, and Mark Willett from the Wannacomet Water Company on Nantucket, MA. The geophysical time-domain electromagnetism (TDEM) work presented in this thesis was completed by Dr. John Lane and Dr. Frederick Day-Lewis.

Abstract

In this study we integrate geophysical, hydrologic, and salinity data to understand the present-day and paleo-hydrology of the Continental Shelf near Nantucket Island, Massachusetts. Time-domain electromagnetic (TDEM) soundings collected across Nantucket and observed salinity profiles from wells indicate that the saltwater/freshwater interface is at least 120 m below sea level in the northern and central portions of the island, far deeper than predicted (80 m) by modern sea level conditions. TDEM soundings also indicate that higher salinity conditions exist on the southern end of the island. These findings suggest a relatively high-permeability environment. Paradoxically, a deep, scientific borehole (USGS 6001) on Nantucket Island, sampling Tertiary and Cretaceous aquifers, is over-pressured by about 0.08 MPa (8 m excess head), which is suggestive of a relatively low-permeability environment. We constructed a series of two-dimensional, cross-sectional models of the paleohydrology of the Atlantic Continental Shelf near Nantucket to understand the flushing history and source of overpressure within this marine environment. We considered two mechanisms for the emplacement of freshwater: (1) meteoric recharge during sea level low stands; and (2) sub-ice-sheet and glacial-lake recharge during the last glacial maximum. Results indicate the sub-ice-sheet recharge from the Laurentide Ice Sheet was needed to account for the observed salinity/resistivity conditions and overpressures. Both TDEM soundings and model results indicate that a lateral transition from fresh to saltwater occurs near the southern terminus of the island due to ice sheet recharge. We also conclude that the overpressure beneath Nantucket represents, in part, “fossil pressure” associated with the last glacial maximum.

Table of Contents

List of Figures

List of Tables

Introduction

Many coastal aquifer systems on the Atlantic Continental Shelf offshore New England, USA have anomalous volumes of freshwater that extend far offshore (>20 km) [Hathaway et al., 1979; Kohout et al., 1977]. These observations are difficult to explain based on modern sea level conditions. On Nantucket Island, Massachusetts, for example, monitoring wells PT-12 and PT-13, installed to 90 and 110 meters below sea level (mbsl), respectively, and well USGS 6001, installed to 514 mbsl, contain groundwater with salinities of less than 1 part per thousand (ppt) within all permeable units (Fig. 1) [Folger et al., 1978]. The observed freshwater below Nantucket is substantially deeper than would be expected based on the Ghyben-Herzberg principle [Drabbe and Badon-Ghyben, 1889; Herzberg, 1901; McWhorter and Sunada, 1977]. Given water-table elevations of about 2 m at wells PT-12 and PT-13, the Ghyben-Herzberg principle predicts that the freshwater/saltwater interface is approximately 80 m below sea level,

$$Z = \frac{\rho_f}{\rho_s - \rho_f} h \approx 40h \ , \qquad (1)$$

where,

Z is depth of the freshwater/saltwater interface below sea level

ρ_f is density of freshwater (1000 kg/m^3)

ρ_s is density of saltwater (1025 kg/m^3)

h is height of the water table above sea level.

This is substantially shallower than the observed freshwater at 514 mbsl within USGS 6001.

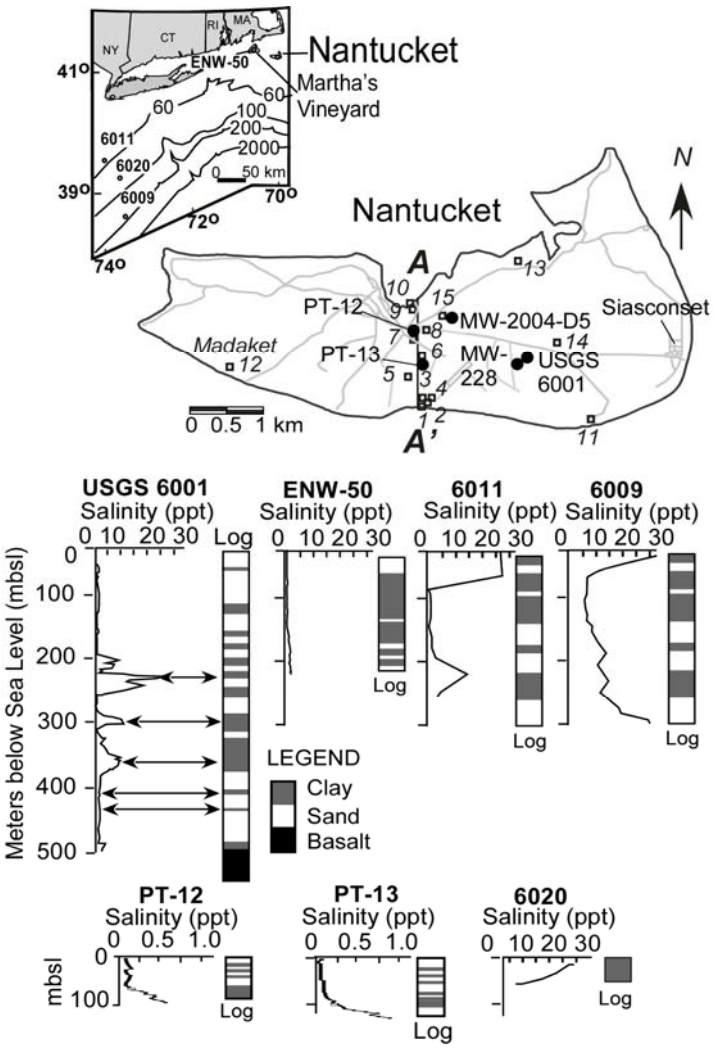

Figure 1. Location of wells on Nantucket Island, Martha's Vineyard Island and the Atlantic Continental Shelf. Numbered squares on the Nantucket map indicate the location of time-domain electromagnetism (TDEM) soundings. Cross section A-A' is associated with the cross section on Figure 6. Salinity profiles are shown of wells on the North Atlantic Continental Shelf. Bathymetry contours are in meters [Kohout et al., 1977; Folger et al., 1978; Hathaway et al., 1979; Hall et al., 1980]. Note the change in scale for wells PT-12 and PT-13

Inspection of long-term water level records from wells located near Nantucket Island's principal well fields in the center of the island reveals no declining trends over the last two decades; hence it is unlikely that this discrepancy results from mining of groundwater by over-pumping. Indeed, the withdrawal rates represent less than 10% of the available recharge on the island. Unexpected freshwater has also been observed on Martha's Vineyard, Massachusetts (to depths of 228 m), and even farther (>100 km) off the New Jersey coast (wells 6009, 6011, 6020) where pore waters with solute concentrations of less than 5 ppt have been noted within Pleistocene, Pliocene, Miocene, and Upper Cretaceous sand units [Kohout et al., 1977; Hathaway et al., 1979; Hall et al., 1980] (Fig. 1).

How and when did freshwater get emplaced within the confined aquifers beneath Nantucket Island? During Pleistocene sea level low stands, hydraulic heads along the Massachusetts coast would have been far too low to drive meteoric water very far offshore [Kooi and Groen, 2001]; moreover, confined aquifers south of Martha's Vineyard and Nantucket outcrop or subcrop below sea level in Nantucket Sound, thus onshore recharge cannot be occurring presently. The fresh and brackish sub-seafloor pore waters that occur along the northeastern U.S. Atlantic coast can be considered key examples of paleo-groundwater that was emplaced during Pleistocene sea level low stands and escaped salinization (e.g., flushing with sea water) during Holocene sea level rise [Hathaway et al., 1979; Meisler et al., 1984; Kooi and Leijnse, 2000; Person et al., 2003]. Several competing mechanisms have been proposed to explain how paleo-groundwater is emplaced during glacial low-stand periods. Early studies considered the shore-normal hydraulic gradient associated with the topography of the Continental Shelf

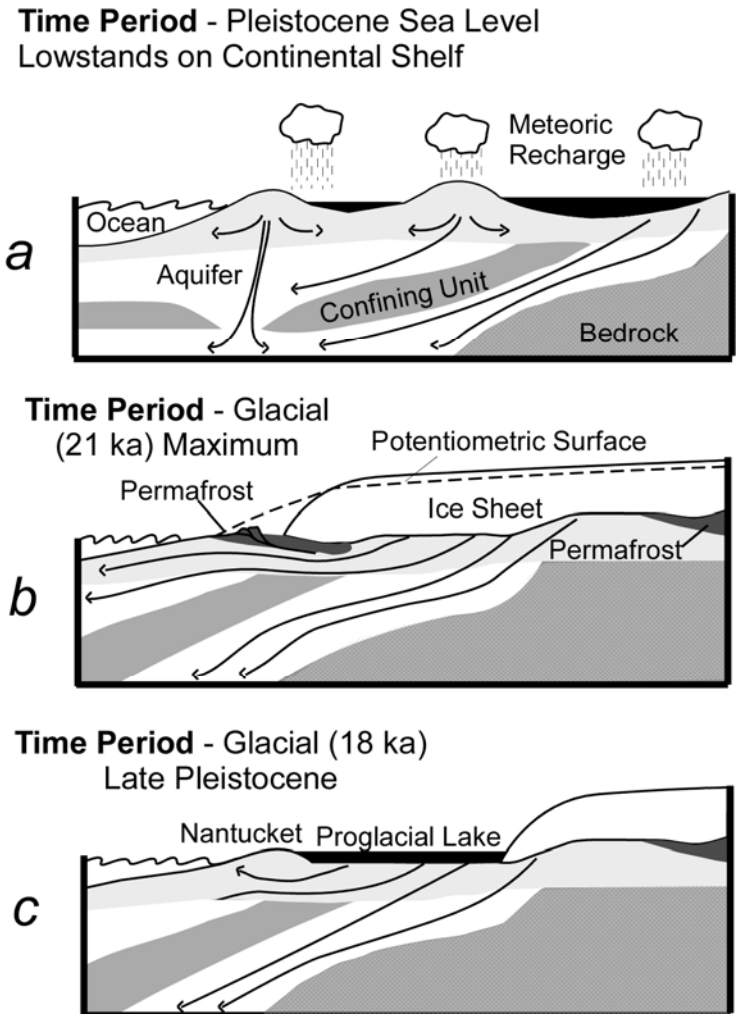

Figure 2. Conceptual models for freshwater plumes: (a) lateral incursion of freshwater during the Pleistocene sea level low stands [Meisler et al., 1984] and vertical infiltration of meteoric water induced by local flow cells on the Continental Shelf [Groen, 2002]; (b) sub-ice-sheet recharge from the Laurentide ice sheet [Person et al., 2003]; (c) infiltration beneath pro-glacial lakes.

as the primary driving force for freshwater recharge during sea level low stands [Meisler et al., 1984] (Fig. 2a). More recently, Groen et al. [2002] argued that local flow systems associated with secondary topography of the subaerially exposed and incised shelf are essential to emplace meteoric water far out onto the Continental Shelf (Fig. 2a), whereas Person et al. [2003] emphasized the role of sub-ice-sheet recharge (Fig. 2b).

Several proglacial lakes formed following the last glacial maximum as the Laurentide ice sheet retreated (Fig. 3) [Uchupi et al., 2001]. Seepage from the proglacial lakes during the last glacial maximum in Nantucket Sound, Cape Cod Bay, Block Island Sound, and Long Island Sound (Fig. 3) could have provided extensive recharge to the confined aquifers of the Continental Shelf of New England. When the southern dams of the proglacial lakes failed, rapid sedimentation on the Continental Shelf would have also changed the land surface morphology, created rapid sediment loading, and perhaps driven infiltration of freshwater [Uchupi et al., 2001] (Fig. 2c). Local recharge could be facilitated by gaps in confining units due to either non-deposition or erosion.

There is evidence that flushing with freshwater has occurred on the Continental Shelf within the deep Cretaceous and Tertiary units on Nantucket during the recent past (USGS 6001, Fig. 1). All permeable Cretaceous and Tertiary units within USGS 6001 contain freshwater; however, the pore waters within the thick low-permeability units show high salinities of up to 12-13 ppt and display vertical solute diffusion profiles. Interestingly, the thin confining units contain low-salinity pore water, which indicates that vertical diffusion of the solutes has already run its course (Fig. 1). This suggests that the Tertiary and Cretaceous sand units once contained high salinity waters and were flushed with fresh groundwater, but diffusive transport of saltwater within the thick, low-permeability

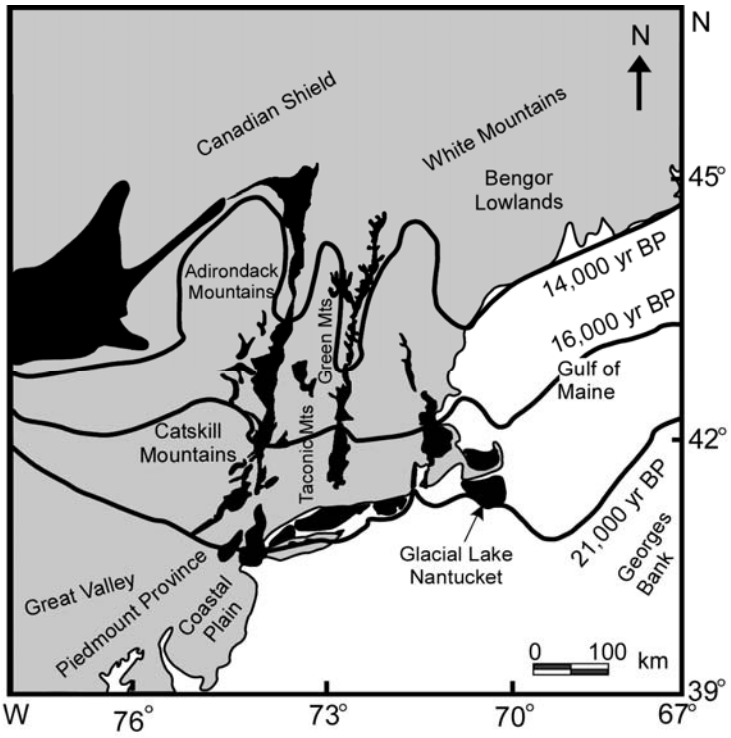

Figure 3. Distribution of proglacial lakes and position of maximum ice sheet extent during the Late Quaternary on the Atlantic Continental Shelf [after Uchupi et al., 2001].

units has not yet reached equilibrium. Simple vertical diffusion models [Person et al., 2003] suggest that the flushing of the Tertiary and Cretaceous aquifers occurred as recently as 21 ka, about the time of the last glacial maximum.

In addition to anomalous amounts of freshwater observed below Nantucket, groundwater elevations measured monthly as part of the National Water Information System for the United States Geologic Survey (USGS) [http://nwis.waterdata.usgs.gov/nwis/gwlevels] have identified elevated hydraulic heads within the deep Tertiary and Cretaceous units at well USGS 6001 on Nantucket. Hydraulic heads within USGS 6001 are overpressured by up to 8m above sea level (0.08 MPa) and 4m above the local groundwater table as shown in USGS 228 (Fig. 4). Smaller overpressure (approximately 0.3 m) was also observed within a 228 m deep well (ENW-60) on Martha's Vineyard [Kohout et al., 1988]. Even based on the water table elevations of 7.5 m above sea level in the deep USGS 6001, the Ghyben-Herzberg principle still under-predicts the amount of freshwater below Nantucket (predicted 300 m versus observed 514 m).

Overpressure observed in the Tertiary and Cretaceous deposits and the anomalous quantities of freshwater within those units represent a paradox. High fluid pressures are typically suggestive of a low-permeability environment whereas the large quantities of freshwater beneath Nantucket are suggestive of a high-permeability system. However, the elevated heads in the Tertiary and Cretaceous aquifers beneath Nantucket may have occurred in the recent past as a result of rapid sedimentation following glaciation. Near-lithostatic overpressures have been inferred offshore New Jersey where sedimentation

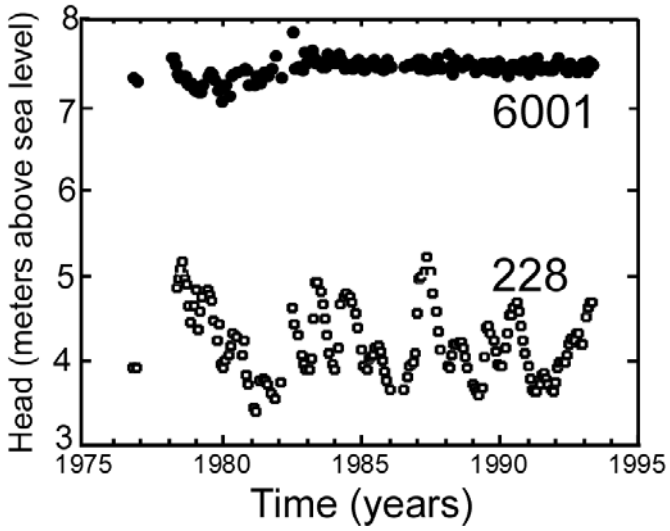

Figure 4. Head data comparing the local water table elevation in well 228 and Cretaceous aquifers in well 6001 beneath Nantucket Island between 1976-1993. The data indicated that the deep aquifers are anomalously pressured and disconnected from the water table flow system. The locations of the wells are shown on Figure 1.

rates were high (~ 1 mm/yr) and confining units are thick [Dugan and Flemings, 2000]. Fluid-flow models by these authors demonstrated how overpressures offshore New Jersey focus fluid migration along permeable sand layers; Dugan and Flemings [2000] argued that Late Pleistocene sedimentation was the sole mechanism responsible for high heads inferred from porosity data and laboratory experiments; however, it is also possible that the high heads are relic features created by extremely high hydraulic heads along the Continental Shelf due to glacial loading.

Modeling Approach and Hypothesis

To date most studies that have developed quantitative models of groundwater flow beneath ice sheets have utilized static representations of ice-sheet geometry and neglected the effects of hydromechanical loading [Boulton et al., 1995; Piotrowski, 1997; Person et al., 2003]; however, if the ice sheet overrides low-permeability sediments, or if rapid sedimentation occurs following glaciation, then hydromechanical effects need to be simulated to account for the effect of loading on groundwater flow [Lerche et al., 1997; Bekele et al., 2003; Lemieux et al., 2006; Person et al., 2007]. Here we use variable-density, cross-sectional models of fluid flow, solute transport, and sediment loading to predict fluid pressures and solute distribution. The hydrostratigraphy represented in this model is based on detailed stratigraphic correlations between available wells on Nantucket Island and Martha's Vineyard, as well as a series of offshore borings. These simulations are compared with time-domain electromagnetic (TDEM) soundings collected from across Nantucket and salinity profiles and hydraulic head pressures from wells on the island.

The working hypothesis for this study is that sea level lowstands associated with Pleistocene sea level variations could not have been the sole mechanism responsible for the excess freshwater and hydraulic heads beneath Nantucket. In this study it is hypothesized that the high hydraulic heads associated with the last glacial maximum and the sediment loading associated with the high sedimentation rate of the Late Pleistocene are at least partially, if not predominately, responsible for the modern distribution of freshwater and hydraulic heads beneath Nantucket.

Purpose of Investigation

In this study we integrate geophysical, hydrologic, and salinity data with numerical modeling to understand the present-day and paleo-hydrology of the Continental Shelf near Nantucket Island, Massachusetts. The purpose of this study is to investigate how Pleistocene sea level variations, last glacial maximum and high Pleistocene sedimentation rates associated with the retreat of Glacial Lake Nantucket may have affected the freshwater and hydraulic head distribution beneath Nantucket. This study helps to unravel the complex paleo-hydrologic history associated with the last glacial maximum and subsequent sea level rise while also providing critical information about the distribution of the potable freshwater resources available to Nantucket Island.

Study Area

Nantucket's demand for potable water has increased significantly over the last two decades due to tourism and development. One new well field has been brought on line (State Forest) in the past decade and another is planned (North Pasture). The majority of Nantucket's municipal potable water is supplied by well fields (PW-12 and PW-13)

located within the central but narrowest portion of the island. This highlights the vital need to understand the distribution of freshwater across the island. Water-table elevations vary across the island from up to 3.5 m above sea level in the widest part of the island to less than 2 m at the narrowest part of the island where municipal wells tap into the island aquifers. The water table declines near the coastline where it is even with modern sea level. Numerical modeling, based on projected pumping increases, indicates that saltwater upconing could occur within municipal water wells before 2014 [Person et al., 1998]; these models however, did not account for the presence of the potentially thick confining glacio-lacustrine deposits from former Glacial Lake Nantucket nor the offshore freshwater. Nevertheless, these studies have led to increased interest in monitoring the distribution of freshwater and saltwater across the island

Basement rocks beneath Nantucket Island consist of Triassic basalts overlain by 460 m of coastal plain sediments of Cretaceous, Tertiary, and Quaternary age [Folger et al., 1978]. Cretaceous sediments on Nantucket range from 118 to 457 mbsl (Fig. 1). The lower portion of that section contains soft, unconsolidated layers of sand and clay, whereas the upper section is mostly clay with interbedded layers of sand [Folger et al., 1978]. Tertiary glauconitic green sand is regionally located above the Cretaceous package; these Tertiary sands have been penetrated by several wells across the island at 80-90 mbsl. Paleontologic studies have linked glauconitic green sand to a similar green sand unit observed on the nearby Martha's Vineyard at a depth of approximately 30 mbsl [Hall et al., 1980]. Folger et al. [1978] inferred 85 m of Pleistocene sediment overlying the green Tertiary sand within borehole USGS 6001. Within the 85 m of Pleistocene sediment, Folger et al. [1978] identified mostly medium-to-coarse grained sand within

several layers containing shell fragments of up to 7 cm across between 28 mbsl and 51 mbsl. The Wannacomet Water Company on Nantucket produces groundwater from these shelly layers. Folger et al. [1978] also describe two zones of either glacial till or weathered soil at 25 and 53 mbsl. Wisconsin-aged glacio-lacustrine deposits of up to 160 m thickness have been identified in Nantucket Sound just north of Nantucket Island [O'Hara and Oldale, 1987]; these deposits consist of mostly silt and clay. Similar glacio-lacustrine deposits were observed throughout the western region of Cape Cod [Masterson et al., 1997]. It is likely that these deposits were part of Glacial Lake Nantucket and likely extend south below Nantucket to the location of the terminal moraine. Portions of this moraine are still present on Nantucket shown by highlands reaching 33 m above sea level in the central eastern portion of Nantucket Island [Oldale, 1985].

Geophysical Data

The time-domain electromagnetic (TDEM) method [Nabighian and Macnae, 1991] is commonly used for groundwater resource evaluation [Fitterman and Stewart, 1986], determination of the depth to the freshwater/saltwater interface [Fitterman and Deszcz-Pan, 1999], and mapping the horizontal extent of saline intrusions [Mills et al., 1988]. A TDEM sounding involves the application of a direct current to an ungrounded transmitting coil, placed at the earth's surface. Thus induces eddy currents in subsurface conductors. The current to the transmitting coil is switched off, and the subsequent decay of the secondary fields produced by the eddy currents is recorded by a receiver coil. These are converted to apparent resistivity versus time data that can be inverted for vertical conductivity structures assuming a layered earth model.

Although the TDEM results are useful for understanding subsurface variations in salinity, the method is limited in two important respects. First, the reliability of TDEM results decreases with depth. The maximum depth of investigation in this study is about 120 m based on sensitivity analysis conducted for inversion results. Second, the TDEM soundings may not resolve thin layers or lenses that pinch out laterally, especially at depth.

Time Domain Electromagnetic Survey Results

TDEM soundings were collected on Nantucket Island at 10 sites in May 2002, and at an additional 6 sites in August 2004 (Fig. 1). A Geonics PROTEM 47[1] system was used with a single-turn transmitter coil. For the 2002 data, we used currents of 2.5 to 3.0 ampere (A) in a 40-m by 40-m transmitter coil. In 2004, we used a current of 2.0 A with a 60-m by 60-m transmitter coil. The receiver coil was coplanar with, and located in the center of, the transmitter loop. The TDEM field data were processed using the commercial software package TEMIX. Sounding data were inverted using 2-, 3-, and 4-layer models computed by the well know ridge regression method of nonlinear inversion [Marquardt, 1963]. Soundings include ultra high frequency (UHF) (between 300 mega hertz (MHz) and 3.0 giga hertz (GHz)) and very high frequency (VHF) (300 MHz to 3000 MHz), measurements. Inversion results were interpreted for the depths to the freshwater/saltwater interface across the island.

TDEM soundings collected along a north-south transect across Nantucket indicate that the freshwater/saltwater interface may be approximately 100 to 120 mbsl below the

[1] The use of trade, product, or firm names in this publication is for descriptive purposes only and does not imply endorsement by the U.S. Government.

surface in the northern and central portions of the island (Fig. 6). Saltwater was identified at shallower depths in the southern portion of the island (35-45 mbsl). The southward shallowing of the saltwater may result from pumping of municipal water supply wells. It is also possible that the freshwater/saltwater interface is shallower along the southern portion of the island because the glacio-lacustrine deposit does not extend that far south and therefore the interface may have equilibrated locally with modern sea level conditions. Based on observations from the Wannacomet Water Company, the northern portion of the island near Nantucket Harbor contains thick low-permeability sediments. These low permeability sediments may be responsible for preserving the deep freshwater/saltwater interface in that area. Interestingly, results from two TDEM locations (Sites 14 and 15 on Fig. 1) indicate at depths of 80 mbsl and 120 mbsl, respectively, a resistivity too high for a sand to be saturated with true seawater. This could be a transition zone or possibly saltwater trapped within a confining unit. It is, however, possible that freshwater exists below these depths as the maximum penetration for the TDEMS soundings is approximately 120 mbsl.

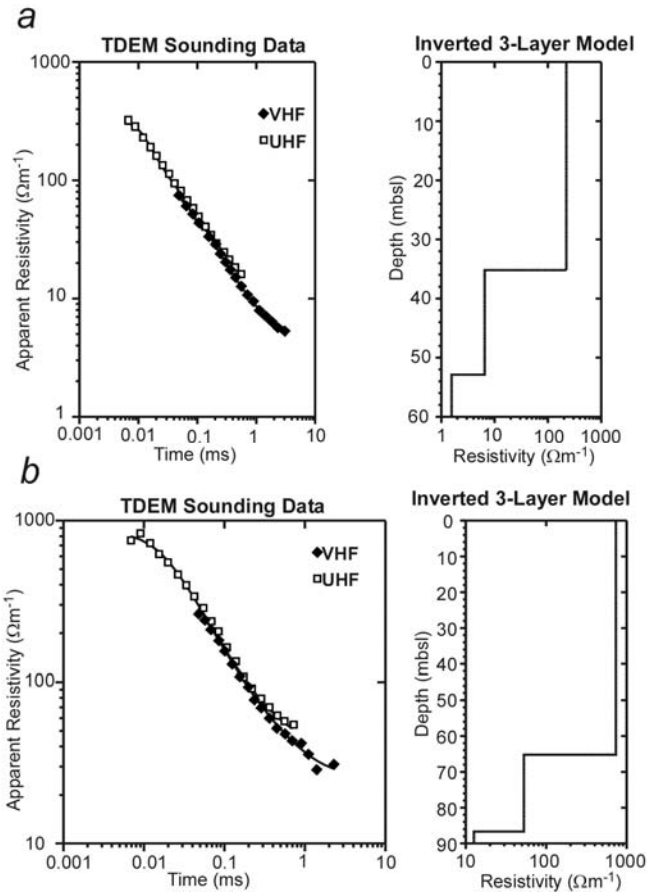

Figure 5. TDEM sounding data and 3-layer inversion results for (a) Site 12 and (b) Site 14 shown on Figure 1. Sounding include ultra high frequency (UHF) and very high frequency (VHF) measurements.

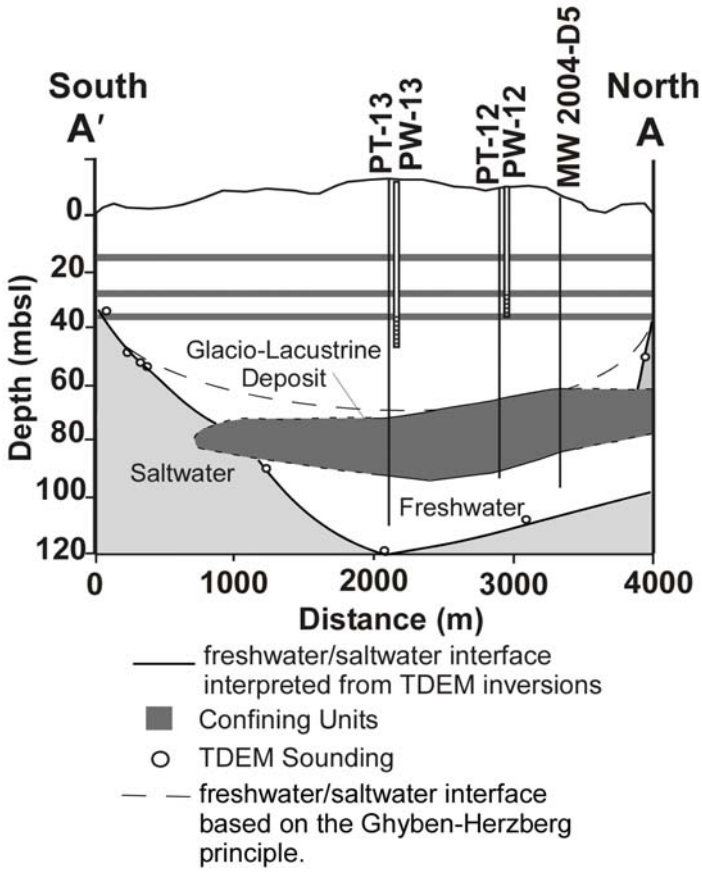

Figure 6. Cross-section across Nantucket Island showing groundwater monitoring wells, PT12, PW-12, PT-13, PW-13 and MW 2004-D5 and the position of the freshwater/saltwater interface estimated by 8 TDEM soundings. The estimated water table elevation and predicted position the freshwater/saltwater interface based using the Ghyben-Herzberg equation (equation 1) is show by a dashed line. The soundings suggest that a lateral transition from fresh to saltwater occurs beneath Nantucket Island from north to south. The location of the cross section is shown on Figure 1.

Mathematical Modeling

We developed a two-dimensional, finite-element model extending from Nantucket Sound to the continental slope approximately 250 km southeast of Nantucket (Fig. 7a). The purpose of the model was to test how sea level changes, rapid sediment loading following deglaciation, and increased groundwater recharge from beneath the Laurentide Ice Sheet and from Glacial Lake Nantucket may have influenced the hydraulic heads and the spatial distribution of fresh groundwater beneath Nantucket. We begin by presenting results that evaluate whether or not sea level oscillations alone could have produced the anomalous freshwater and hydraulic heads observed beneath Nantucket. We then consider what impact the Laurentide Ice Sheet and Glacial Lake Nantucket may have had on this system.

Numerical Methods

The governing groundwater flow equation used to quantify the Pleistocene hydrogeology of the Atlantic Continental Shelf in New England is,

$$\nabla \cdot \left[\rho_{\mathrm{f}} \mathbf{K} \mu_{\mathrm{r}} \left(\nabla h + \rho_r \nabla \mathrm{z}\right)\right] = S_s \rho_o \left[\frac{\partial h}{\partial t} - \frac{\rho_{ice}}{\rho_f}\frac{\partial \eta}{\partial t} - \frac{\rho_s - \rho_f}{\rho_f}\frac{\partial L}{\partial t}\right], \qquad (2)$$

where,

t is time

∇ is the nabla operator

K is the hydraulic conductivity tensor

h is equivalent freshwater hydraulic head

ρ_{ice} is ice density

ρ_s is bulk sediment density

L is the elevation of the sediment-water interface

ρ_r is the relative fluid density

ρ_f is the fluid density

η is the elevation of the top of the ice sheet

S_s is the specific storage.

The relative fluid density, viscosity, and hydraulic conductivity are,

$$\rho_r = \frac{\rho_f - \rho_o}{\rho_o}, \tag{3a}$$

$$\mu_r = \frac{\mu_f}{\mu_o}, \text{ and} \tag{3b}$$

$$\mathbf{K} = \frac{\mathbf{k}\rho_o g}{\mu_f}, \tag{3c}$$

where,

ρ_o and μ_o are the reference density and viscosity at standard state (0 MPa, 0.0 mg/liter dissolved solids), respectively

k is the permeability

μ_f is the water viscosity

K is hydraulic conductivity

g is the acceleration due to gravity.

Equation 2 is capable of representing groundwater flow induced by water table gradients, spatial variations in subsurface fluid density as well as sediment and ice-sheet loading [Person et al., 2007].

Thermodynamic equations of state are required to compute the density and viscosity of groundwater at elevated temperature, pressure and salinity conditions. We assume isothermal conditions for these cross-sectional model runs. This assumption is warranted given that the sedimentary column is relatively thin (<1200 m). We use the equations of state of Kestin et al. [1981] that are capable of representing fluid density and viscosity.

Transient, advective-dispersive solute transport in this model is represented by:

$$\nabla \cdot \left[\mathbf{D} \nabla C\right] - \vec{v} \cdot \nabla C = \frac{\partial C}{\partial t} \ , \tag{4}$$

where C is solute concentration, v is the seepage velocity (x- and z-directions) and **D** is the advection-dispersion tensor for the porous medium. Equation 4 neglects the effects of solute transport due to porosity changes associated with sediment and ice-sheet loading which are expected to be small.

The Darcy flux used in the solute transport equation was computed using a variable-density formulation,

$$v_x = -\frac{K_x}{\phi} \mu_r \frac{\partial h}{\partial x} \quad \text{, and} \tag{5}$$

$$v_z = -\frac{K_z}{\phi} \mu_r \left[\frac{\partial h}{\partial z} + \rho_r \right], \tag{6}$$

where K_x and K_z are principal components of the hydraulic conductivity in the x and z directions and ϕ is porosity.

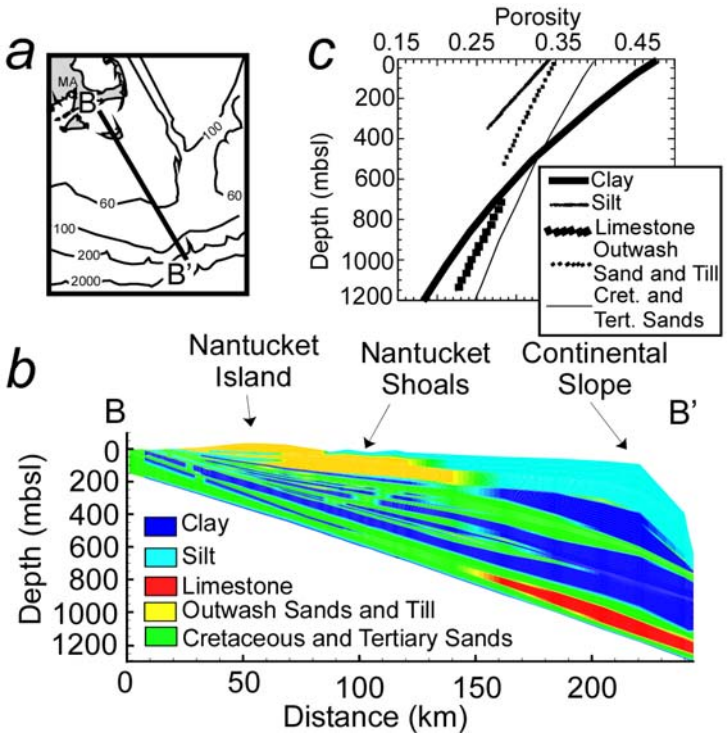

Figure 7. (a) The location of cross section used in the cross-sectional model. The contours are in mbsl. (b) Stratigraphy of the cross section. (c) Porosity depth relationship for each stratigraphic unit described in (b).

The components of the advection-dispersion tensor are given by [Bear, 1972],

$$D_{xx} = \alpha_L \frac{v_x^2}{|v|} + \alpha_T \frac{v_z^2}{|v|} + D_s$$

$$D_{zz} = \alpha_T \frac{v_x^2}{|v|} + \alpha_L \frac{v_z^2}{|v|} + D_s \text{ and} \qquad (7)$$

$$D_{zx} = D_{xz} = (\alpha_L - \alpha_T)\frac{v_x v_z}{|v|},$$

where,

α_L is the longitudinal dispersivity

α_T is the transverse dispersivity

$|v|$ is absolute value of the groundwater velocity ($|v| = \sqrt{v_x^2 + v_z^2}$)

D_s is the solute molecular diffusion coefficient.

The solute transport and flow equations are formally coupled through the equations of state for fluid density and viscosity; however, the non-linearity is relatively weak and the two equations can be solved separately and sequentially while stepping through time.

Boundary conditions for the groundwater flow equation include a 'specified head' (water-table) condition at the Earth's surface and no-flow boundaries along the bottom and sides of the solution domain. The 'specified head' condition varies in time depending on sea level, topography, and glacial position. Boundary conditions for solute transport equations include a constant concentration of 0.0 or 35 ppt depending on whether the local land-surface elevation is above or below sea level. No solute flux boundary conditions were imposed along the sides and base of the sedimentary basin.

The fluid flow equation is solved by the finite-element method. We solve the solute transport equation using the modified method of a characteristics algorithm [Zheng and Bennet, 1995]. Three-node triangular elements are used to discretize the solution domain and the resulting set of algebraic equations is solved using Gaussian elimination. The solution domain is discretized using 12,030 triangular elements composed of 6,167 nodes. The elements size in the x-direction varies between about 300 m in the western portion of the mesh in the vicinity of Nantucket, to 22 km in the eastern portion of the mesh near the continental slope. Element size in the z-direction varies between less than 1 m and approximately 300 m. We refined the grid within confining units to minimize numerical dispersion. The number of nodes in each vertical column ranges between 18 and 92.

Numerical Mesh

The stratigraphy of the cross-section is based on boring logs on Nantucket [Kohout et al., 1977], Atlantic Coring Margin Coring project (AMCOR) wells [Hathaway et al., 1979], and Continental Offshore Stratigraphic Tests (COST) wells G-1 and G-2 located in Georges Bank east of Cape Cod [Taylor and Anderson, 1982; Schlee and Fritsch, 1982] and COST wells B-2 and B-3 located approximately 120 km south of Long Island, NY [Scholle, 1977 and Scholle, 1980]. The stratigraphy was divided into five types of sediment including Tertiary and Cretaceous sands, shallow outwash sands, silts, clays, and limestone (Fig. 7b) which consist of a wide range of porosities and permeabilities. We do not represent the sand and clay as being continuous as we found a lack of lateral correlation between aquifers and confining units among closely spaced wells (e.g., ENW-50 and USGS 6001). Porosity and permeability had to be assigned to

each unit. Over the depth range considered (1.2 km) these properties can vary considerably, even within a lithologic unit due to mechanical compaction and diagenetic processes associated with burial; these effects can amount to orders-of-magnitude changes in the permeability of the sediment at depth. Although the relationship between porosity and permeability is complex, a compilation of data by Neuzil [1994], Lucia [1995] and Shenhav [1971]) has shown a distinct log-linear trend between permeability and porosity for porosities. Many studies have used this log-linear relationship within their numerical models [Corbet and Bethke, 1992; Garven, 1989]. We assume the log-linear relationship between porosity and permeability,

$$\log_{10}(k_{max}) = a + b\phi, \tag{8}$$

where k_{max} is the maximum permeability in a lithologic unit, ϕ is porosity and a and b are empirical coefficients [Table 1]. To apply this relationship, it is necessary to assume a compaction curve within the sediment. We relate porosity to effective stress and compressibility using a relationship presented by Hubbert and Rubey [1959] and Bethke and Corbet [1988],

$$\phi=\phi_o e^{(-\beta\sigma e)}, \tag{9}$$

where ϕ_o is the initial porosity

ϕ is the porosity at the maximum effective stress

β is the bulk compressibility of the sediment

σ_e is the effective stress.

However, equation 9 assumes that all porosity loss can be uniquely tied to effective stress (σ_e). This equation does not take into effect porosity losses associated with diagenetic

effects while are generally dependent on temperature, pressure chemical environment and time. However, since our cross sections is relatively shallow and young, diagenetic effects are likely minimal. In addition, this equation assumes that the porosity-effective stress relationship is elastic. This assumption is reasonable because sediments with the cross section are at low temperatures and pressures and are not well consolidated. The σ_e can be calculated based on Terzaghi's principle,

$$\sigma_e = \sigma_v - P, \tag{10}$$

where σ_v is the total vertical stress or overburden stress and P is the pore pressure. The pore pressure, assuming hydrostatic conditions is,

$$P = (h-z)\rho_o g, \tag{11}$$

where h is the hydraulic head, z is the depth and ρ_o is the base density of the fluid. The total vertical stress or overburden stress is estimated by,

$$\sigma_v = g\int_z [\rho_s(1-\phi) + \rho_f \phi]dz, \tag{12}$$

where ρ_s is the bulk density of the sediment and ρ_f is the density of the fluid.

Compressibilities, initial porosities and the a and b parameters used in the permeability-porosity relationship are shown on Table 1. Porosity-depth profiles are shown on Fig. 7c. A specific storage of 8.0 x 10^{-5} m^{-1} was applied to clays, while 8.0 x 10^{-6} m^{-1} was used as the specific storage of the other more permeable units. Using these relations permeability ranged in the clay units from 8.3 x 10^{-19} m^2 to 9.7 x 10^{-20} m^2. Cretaceous and Tertiary sand permeability ranged from 9.1 x 10^{-13} m^2 to 1.0 x 10^{-13} m^2. Shallow outwash sand and glacial till permeability ranged from 8.7 x 10^{-14} m^2 to 5.0 x 10^{-14} m^2, and silt permeability ranged from 2.9 x 10^{-16} m^2 to 1.0 x 10^{-16} m^2. Specific storage

Table 1. Input parameters for porosity, permeability and effective stress relationships

Sediment Type	Compressibility m^2/N	Φ_o[a]	a[b]	b[b]
Clay	$8.0x10^{-8}$	0.48	-20	4.0
Silt	$8.0x10^{-8}$	0.35	-17	4.2
Tertiary and Cretaceous Sands	$4.0x10^{-8}$	0.40	-15	7.4
Shallow Outwash Sands and	$4.0x10^{-8}$	0.35	-16	8.4
Glacial Till	$5.0x10^{-8}$	0.40	-17	5.0
Limestone				

[a]Initial porosity of the sediment

[b]a and b parameters used in the permeability-porosity relationship in equation 8.0

and permeability parameters are consist with published values each sediment type [Freeze and Cherry, 1979].

It has been suggested that confining units beneath Nantucket have undergone deformation as a result of glacio-tectonic activity associated with the advancement of the Laurentide Ice Sheet [Oldale and O'Hara, 1984]. Oldale and O'Hara [1984] identified Cretaceous units which have been thrusted laterally by as much as 1.5 km on Nantucket. Boulton and Caban [1995] described how high pore pressure and low effective stress are frequently associated with glacio-tectonic features such as those observed on Nantucket Island. It is possible that thrust faulting has created permeability conduits through deep confining units beneath Nantucket that are not represented in our model.

Glacial Lake Nantucket catastrophically drained approximately 17,000 years ago [Uchupi et al., 2001]. This would have released large volumes of sediment that could have resulted in high sedimentation rates on the shelf and massive debris flows on the outer shelf and slope [Uchupi et al., 2001]. This period of rapid sedimentation was simulated in our model by allowing a portion of the upper Pleistocene elements in our mesh to grow until it attained modern Pleistocene elevations after the Laurentide Ice Sheet retreated. We updated the concentration and hydraulic heads of the top nodes using the sea level elevation, land surface elevation, and ice sheet thickness. Although actual sedimentation rates immediately following the drainage of Glacial Lake Nantucket are unknown, the majority of glacial lakes associated with the Laurentide Ice Sheet drained within 4,000 years of Glacial Lake Nantucket [Uchupi et al., 2001]; therefore, we allowed our mesh to grow to modern topography for 4,000 years from 17,000-13,000

years ago. Sedimentation rates within the simulation during that time ranged from 0 m/yr to 0.055 m/yr depending on where deposition was observed on the cross-section (Fig. 8). Sedimentation rates were highest near the continental slope where Pleistocene sediments were the thickest.

Hydrologic Stresses and Model Input

Variable Sea Level Simulation

The first model is constructed to test the hypothesis that sea level variations alone could produce the excess heads and anomalous freshwater beneath Nantucket. Pleistocene sea level varied by as much as 120 m with a period of 40,000 years to 100,000 years and an average sea level of approximately 40 m below modern sea level [Shackleton, 1987; Raymo et al., 1989, 1997; Vail and Hardenbol, 1979; Summerhayes, 1986; Haq et al., 1987; Shackleton and Opdyke, 1973; Hays et al., 1976; Clark, 1994; Imbrie, 1985; Peltier, 1998]. A sea level boundary condition is applied during the simulation using a sine curve with an amplitude of 60 m, a period of 100,000 years, and set so that average sea level during the Pleistocene would have been 40 m below modern. Sea level during glacial maximum is set to 120 mbsl. A local sea level curve for New England [Redfield and Rubin, 1962; Oldale and O'Hara, 1980; Gutierrez et al., 2003] was used from 16 ka to present (Fig. 9). It is necessary to apply a variable sea level curve for the entire length of the Pleistocene, as opposed to using a shorter simulation time with only 3 or 4 sea level cycles, to allow the cross section to better equilibrate with the initial salinity concentrations that were emplaced at the start of the simulation. An initial sea water salinity condition was assigned to deep Tertiary and Cretaceous sand and clay units while shallower outwash sands and silts were assigned fresh pore waters. Had sea level

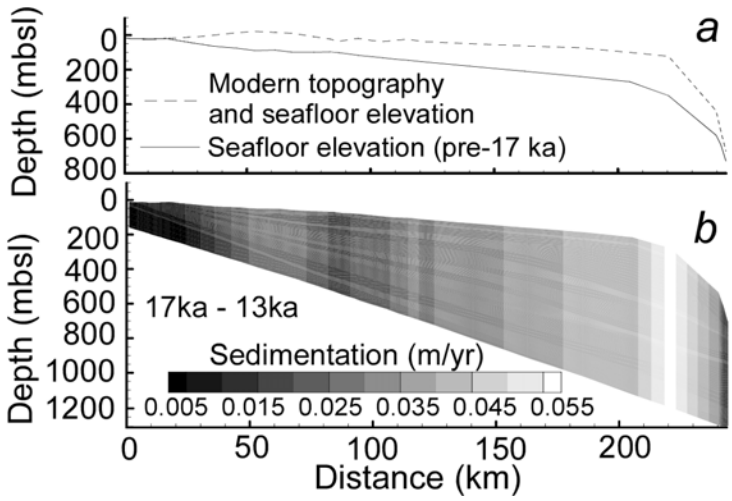

Figure 8. The change in Continental Shelf elevation between 17 ka and present. (a) Comparison of pre-17 ka topography and modern topography and seafloor elevation of the cross section. (b) Sedimentation rates from 17ka to 13 ka along the cross section.

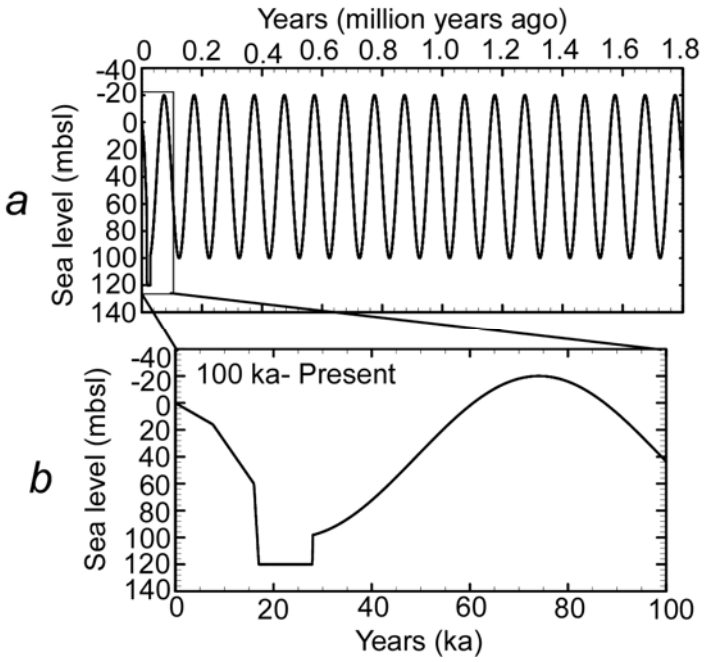

Figure 9. (a) Pleistocene sea level curve represented using a sine function with an amplitude of 60 m and a period of 100,000 years. (b) Sea level was set to 120 mbsl for glacial maximum. A local sea level curve was used for 16 ka to present [Redfield and Rubin, 1962; Oldale and O'Hara, 1980; Gutierrez et al., 2003].

only been allowed to cycle 3 or 4 times, it would have been difficult to get mixing between the deep salty Tertiary and Cretaceous units and the shallow freshwater units without using unreasonably high permeabilities for each unit. An initial hydrostatic head boundary condition (consistent with local topography) was used to initial heads for the flow equation. The simulation was run for a total of 1.8 million years to reconstruct the Pleistocene and Holocene hydrologic conditions (Fig. 9a).

Ice Sheet Simulation

Our second model incorporates the effects of the ice sheet and glacial lake boundary conditions during the last 21 ka. The thickness of the ice sheet was estimated using a polynomial expression presented by van der Veen [1999],

$$\eta = H\sqrt{\left[\frac{1-x}{L_{ice}}\right]^2} + z_{ls} \tag{13}$$

where,

H is the maximum ice-sheet thickness at a particular time step

L_{ice} is the ice sheet length at that time step

x is the distance from the margin of the basin

z_{ls} is the local elevation of the land surface

η is ice-sheet elevation above sea level at distance x from the margin of the basin.

The advance of the ice sheet is represented such that the ice sheet builds up slowly from 28 ka to the glacial maximum at 20 ka (Fig. 9a). The ice sheet remains at the glacial maximum from 20ka to 18ka. The ice sheet is allowed to retreat at 18 ka. As the glacier retreats, Glacial Lake Nantucket forms and is present until17 ka, after which it

drains (Fig. 10a) [Uchupi et al., 2001]. During the simulation, the ice sheet attains a maximum thickness of 1800 m for our section, which is consistent with maximum ice sheet thicknesses estimated for southern New England [Denton and Hughes, 1981]. The glacier is allowed to extend 70 km along the cross section to the central portion of Nantucket (Fig. 10b). This is consistent with the established moraine observation that is on Nantucket. While the glacier is present, we apply a specified-head boundary condition along the top boundary assuming that the head at the base of the glacier is equal to 90% the local ice sheet elevation due to fluid-ice density differences [Boulton et al., 1995; Person et al., 2003]. A hydraulic head of 10 m above sea level was applied as a boundary condition when Glacial Lake Nantucket was present (Fig. 10b) [Uchupi et al., 2001]. The loading and head caused by the glacier and glacial lake affect the effective stress within the underlying sedimentary layers; the changes in effective stress will change the porosity (Eq. 10) and permeability (Eq. 8). We permitted infiltration to exceed the local melting rate due to the effects of up-gradient esker systems [Shreve, 1985].

It has been suggested that shallow permafrost conditions existed along the margin of the Laurentide Ice Sheet in New England [Oldale and O'Hara, 1984]. The permafrost would have significantly decreased the permeability of those sediments [Person et al., 2007]. To replicate the permafrost, the permeability of the upper boundary nodes which are above sea level but not located below the ice sheet is decreased to 10^{-20} m^2 during the advance of the ice sheet and during the glacial maximum. This approach represents a simplification of the actual heat transfer involved during freezing and thawing of permafrost [Person et al., 2007]. The ice sheet simulation was run for 1.8 million years

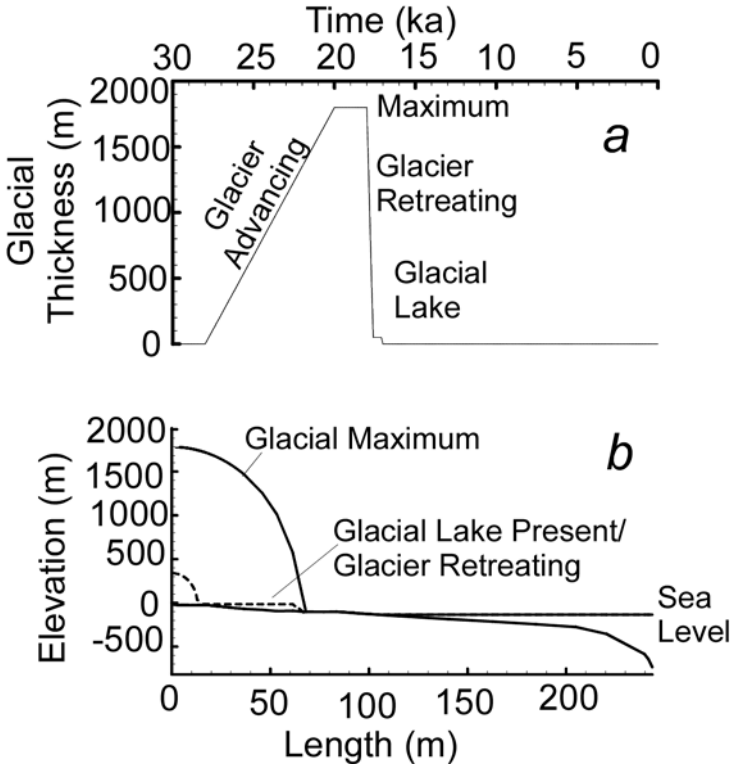

Figure 10. (a) Timing of the advance and retreat of the ice sheet and glacial lake. (b) The elevations of the ice sheet, glacial lake, early Pleistocene topography and sea level while the ice sheet or glacial lake is present.

using the same sea level variations used in the sea level simulation (Fig. 9). The salinity profile from USGS 6001 on Nantucket and the results of the TDEM experiments were used as ground truth for comparison with our numerical experiments.

We ran over 50 simulations using a range of different permeabilities, porosities, compressibilities and specific storages representative of Continental Shelf deposits to better understand what parameters controlled overpressure and salinity distributions on the shelf. Because the permeability, porosity and compressibility are closely linked by equations 8, 9 and 10 it is difficult to describe the ranges of parameters that were tested in our model. However, a relatively narrow range of parameter values were able to produce both the observed salinity distribution and excess heads. Initial clay permeabilities tested ranged from 1.0×10^{-16} m^2 to 1.0×10^{-21} m^2, while initial sand permeabilities tested ranged from 1.0×10^{-11} m^2 to 9.0×10^{-14} m^2. Compressibility and the initial porosity of each sediment type were calibrated so that their porosity depth curves (Fig 7c) were similar to the sediment porosity depth curves compiled by Giles [1997]. Below we represent one set of parameters that we found was consistent with the observed data. We consider the appropriateness of these parameters in the discussion section.

Constant Sea Level Simulation

A third simulation was constructed in which the cross-sectional model is permitted to equilibrate for 1.8 million years with modern sea level conditions (referred to herein as the 'constant sea level' simulation). Here the cross sectional model was run using both the modern topography (i.e. sediment loading associated with the Late Pleistocene was not included in this simulation) and a modern sea level to predict salinity distribution for the Atlantic Continental Shelf.

Results

Solute concentrations using surface boundary conditions that only represent the effects of sea level fluctuations (referred to herein as the 'variable sea level' simulation) indicate that freshwater is only located within shallow sediments (<100 m) on Nantucket and at even shallower depths on the southern side of the island (Fig. 11a). Permeable units at depths of greater than 200 m contain solute concentrations of greater than 10 ppt and are not consistent with the solute concentrations observed within USGS 6001 or interpreted from TDEM soundings. The emplacement of freshwater in deep confined aquifers was only preserved in Nantucket Sound within 20 km of where the confined aquifers outcropped. This conclusion was reached regardless of the permeability/porosity parameters selected from the 50 simulations we completed. These results indicate that meteoric flushing of the Atlantic Continental Shelf during the sea level lowstands of the Pleistocene cannot be the sole mechanism responsible for the distribution of freshwater beneath Nantucket.

The simulations which include sub-ice-sheet recharge and glacial lake recharge (referred to herein as the 'ice sheet' simulation) show significant flushing beneath Nantucket compared to the variable sea level simulation (Fig. 11b). Freshwater of solute concentrations of less than 1 ppt are predicted within permeable units at depths greater than 300 mbsl. Deep low permeability clays exhibit solute concentrations with diffusional profiles similar to that shown in USGS 6001. Simulations indicate that a small tongue of slightly saltier (salinity ~6 ppt) water invades into the shallow subsurface (<200 m) on the southern end of the island; this is qualitatively consistent with the TDEM results, which similarly indicate that saltwater is found at shallower depths on the southern side

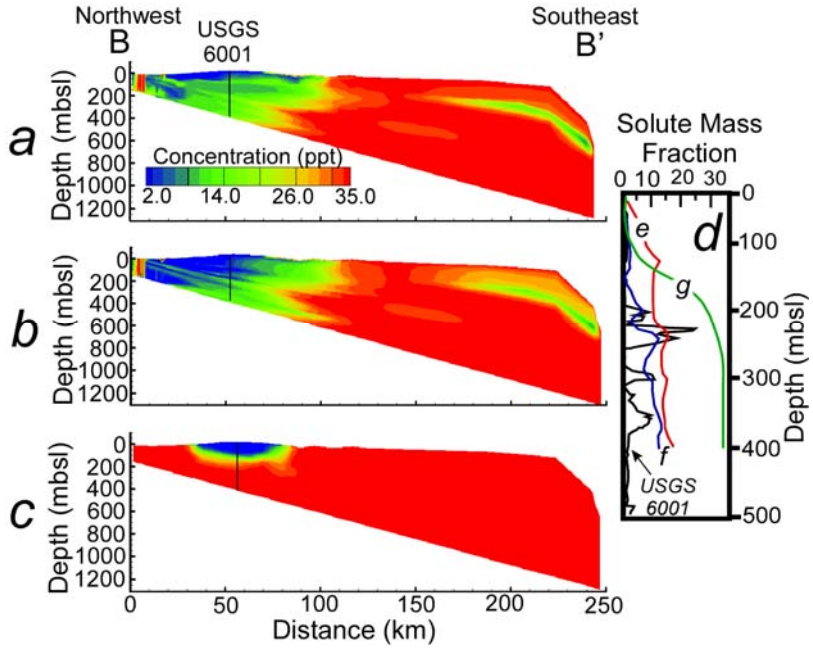

Figure 11. (a) Present-day salinity concentrations from the variable sea level simulation (b) ice sheet simulation and (c) constant sea level simulations. (d) Comparison of solute profiles from the variable sea level (e), ice sheet (f), constant sea level (g) simulation with the observed solute profile from USGS 6001 well. The lateral position of the salinity-depth plot is indicated on Fig. 11a-c by the black line segment. The location of the cross section is shown on Figure 7.

of the island. Thus, the higher salinity conditions here may result from paleohydrologic conditions rather than recent pumping of nearby municipal wells. Our models suggest that the transition between fresh to saltwater exists near the southern end of the island.

For comparison, we also present the constant sea level simulation. This simulation resulted in seawater salinity within pore spaces of sediments everywhere on the Continental Shelf that is below sea level today. Only beneath Nantucket Island was freshwater found. Results are consistent with the Ghyben-Herzberg approximation where the freshwater/saltwater interface beneath Nantucket is located at approximately 120 mbsl (Fig. 11c).

As noted above, the deep Cretaceous and Tertiary aquifers on Nantucket are observed to be overpressured by up to 0.08 MPa (8 m above sea level). The observed overpressures cannot be explained by topographically driven flow, for lack of sub-aerial recharge from the mainland. Computed freshwater heads within deep permeable sediments from the variable sea level simulation varied between -0.5 and 2.3 m in different sand lithologic units beneath Nantucket Island (Fig. 12); these anomalous heads were generated, in part, by Late Pleistocene sedimentation. Results of the ice sheet simulation produce heads that vary from 4.5 to 25.4 m (Fig. 12). Negative computed heads are due to: (1) an imposed sea level boundary condition which is significantly lower than modern levels, and (2) a Continental Shelf aquifer system has not fully equilibrated to modern sea level conditions. Since the USGS 6001 well is open to all units below 120 mbsl, the observed overpressure at that well represents the average of all permeable units below 120 mbsl. The average freshwater hydraulic heads for these Cretaceous and Tertiary aquifers from the variable sea level simulation was only 0.56 m.

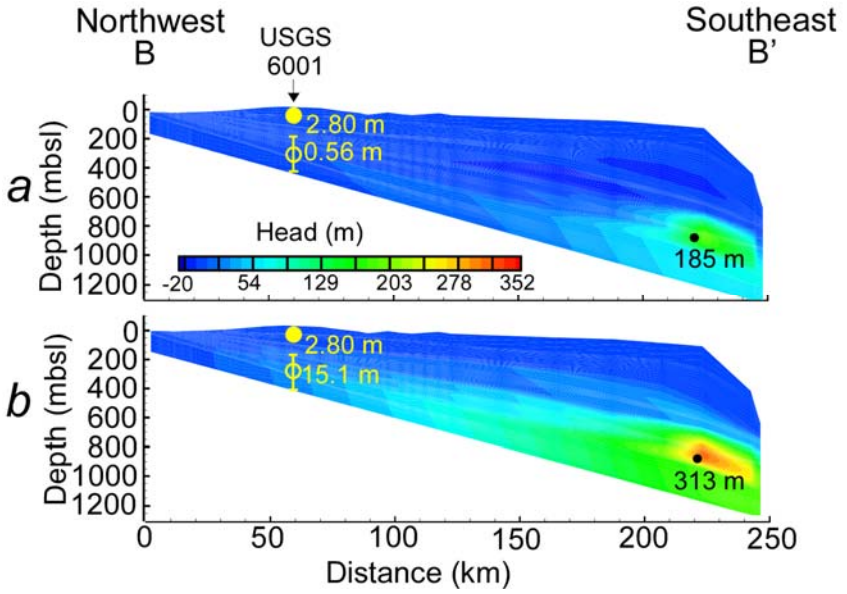

Figure 12. (a) Computed equivalent freshwater hydraulic head from the variable sea level simulation and (b) ice sheet simulation. Hydraulic heads are reported in meters above sea level. Solid circles represent pressure heads at specific location. Open circles represent average pressure heads over the length of only the permeable lithologies. The location of the cross section is shown on Figure 7.

Because shallow water-table elevations across Nantucket are approximately 3 m above sea level, no overpressure would be observed in USGS 6001 in this simulation. However, the average freshwater head from those units in the ice sheet simulation is 15.1 m; this would produce overpressures in USGS 6001 that are 11 m above the local water table, a value that is similar (though not identical) to the observed 4 m of overpressure in that well.

Discussion

These modeling results indicate that sediment loading associated with the high sedimentation rates of the Late Pleistocene was not solely responsible for the overpressure observed beneath Nantucket. Hydraulic heads within sediment below the continental slope are pressured by up to 126 m more within the ice sheet simulation compared to the sea level only simulation (Fig. 12). Given that both simulations were subjected to the same sediment loading, the additional overpressures predicted within the ice sheet run must have originated from the diffusion of high hydraulic heads from the adjacent aquifers during ice-sheet glaciation. The observed excess heads (USGS 6001) thus are inferred to be preserved, fossil hydraulic heads associated with the ice-sheet loading during the last glacial maximum. In their sensitivity study of ice sheet loading within sedimentary basins, Person et al. [2007] and Bense and Person [2006] observed this phenomenon.

The preservation of excess head is illustrated by plotting temporal variations in head during the Pleistocene (Fig. 13) for our ice-sheet simulation. Hydraulic heads remained low throughout the cross section under normal sea level conditions (Fig. 13a). Hydraulic heads within the aquifers below Nantucket became over-pressured by up to

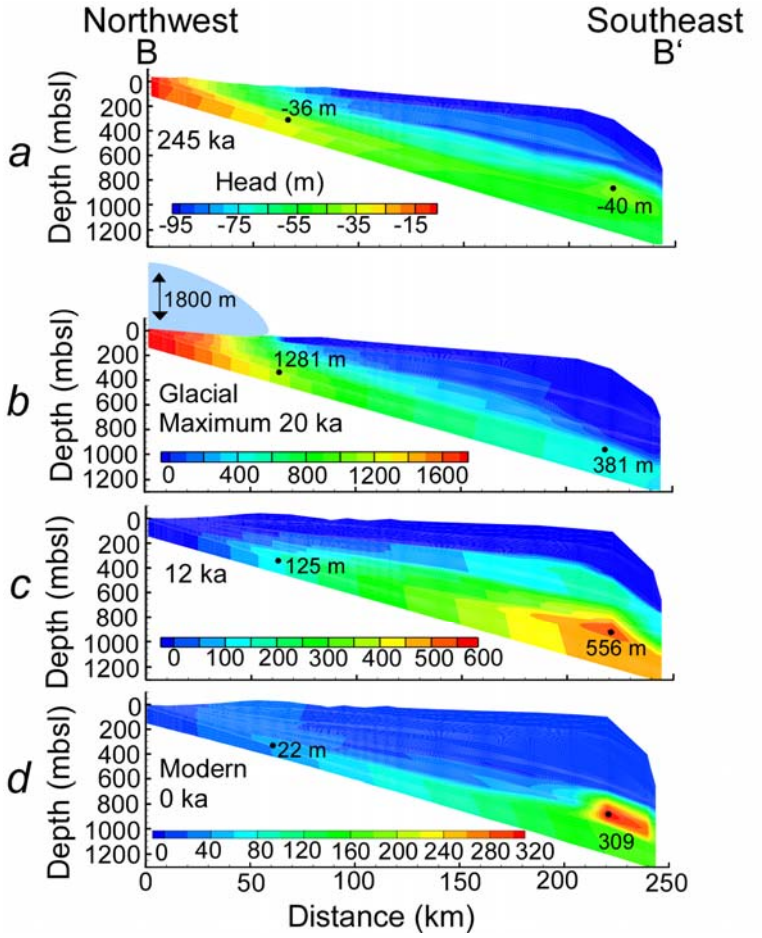

Figure 13. The evolution of hydraulic heads through time in the ice sheet simulation. (a) Hydraulic head at 245 ka. (b) Hydraulic head at glacial maximum 20 ka. (c) Hydraulic head at 12 ka. (d) Hydraulic head at modern 0 ka. The thickness of the sedimentary pile changes between (b) and (c) due to rapid sedimentation associated with the breaching of Glacial Lake Nantucket at 17 ka. Note the change in scale in each plot. The location of the cross section is shown on Figure 7.

1281 m (Fig. 13b) while the ice sheet was present. The lateral transfer of this pressure decreased the effective stress within sediments that were experiencing less overburden pressure (i.e. areas not covered by ice). The decrease in effective stress then caused an increase in the effective permeability of the sediment and allowed high pressure to transfer into even deeper sediment below the continental slope. Deep aquifers near the continental slope became pressured by up to 381 m as the ice sheet reached its maximum extent on the Continental Shelf (Fig. 13b). At that point the high fluid pressures diffused into the surrounding clay units. After the ice sheet retreated, the low permeability clays retained elevated fluid pressure. Fluid pressures subsequently increased due to sediment loading associated with the drainage of Glacial Lake Nantucket and the retreat of the ice sheet. Fluid pressures reached a maximum of 556 m within clay units below the continental slope (Fig. 13c). After sedimentation ceased (approximately 12,000 years ago), heads within the confining units on the slope slowly dissipated while some of the elevated heads also got transferred back beneath Nantucket (Fig. 13d).

It is also interesting to note that effective stresses below Nantucket decreased to zero while the ice sheet was present. This may have allowed thrust features to form associated with the advance of the ice sheet. Ice sheet thrust features were observed on Nantucket Island and Martha's Vineyard by Oldale and O'Hara [1984]. These thrust faults may have helped transport glacial melt water into deeper aquifers below Nantucket.

We can calculate a response time for the clay to predict the time required for the high hydraulic heads to diffuse out of the clay:

$$\tau = \frac{L_{sed}{}^{2} S_S}{K} \tag{14}$$

where

L_{sed} is the length or thickness of the sediment unit

S_S is the specific storage of the confining unit

K is the hydraulic conductivity of the sediment

τ is the response time.

Permeability can be converted to hydraulic conductivity using equation 3c. Based on the thickness of the deep clay unit, approximately 275 m, the S_S of 8.0×10^{-5} m^{-1} and a hydraulic conductivity of 10^{-12} m/s, the time to dissipate the excess head would be approximately 200,000 years. This means that high heads emplaced within the clay units during glacial maximum would not have had enough time to dissipate and equilibrate with modern sea level conditions and therefore would retain a fossil head. These high head pressures in the deep clay units can laterally transfer pressure through deep permeable sand units to beneath Nantucket. Although the computed heads beneath Nantucket Island are about twice as large, it does show that there is high potential for thick low permeable units on the continental slope to transfer fossil pressures to the near shore environment.

Based on the completed simulations, the numerical model is most sensitive to permeability, initial porosity, and compressibility, particularly in the clay and sand units and the last Pleistocene sediment loading rate. Overpressures generated within the cross section were predominately controlled by the sedimentation rates and the permeability of

the clay units. Flushing of freshwater beneath Nantucket was predominately controlled by the permeability of the sand units. Had we raised the permeability or lowered compressibility of the confining units by an order of magnitude, the confining units would have flushed too much and simulations would not reproduce the salinity profiles and observed overpressures beneath Nantucket Island. Although the permeability of the sediment units is reasonable, it may have been possible to obtain similar results using a different cross section where clay units where thicker and the permeability of the clay was higher. Lack of well data in the area of the cross section has made it difficult to predict the stratigraphy and continuity of the units especially at depth. The stratigraphy at depth is based on wells located in Georges Bank, located 200 km east-southeast and wells near the continental slope, 200 km southwest of Nantucket. Therefore, it was decided to only model the shallower (<1200 m) section where we had better well constraints. The sediment column near Georges Bank and on the continental slope south of Long Island is much thicker (> 5000 m) with up to 2000 m of shale [Taylor and Anderson, 1982; Schlee and Fritsch, 1983, Scholle, 1977; Scholle, 1980]. It is possible that these deep shales are highly overpressured and that if we deepened our cross section to include these units, we might have found that they also contribute to overpressure observed beneath Nantucket. This could have led us to use a higher permeability for the shallower clay units.

Conclusion

Our study demonstrates the utility of integrating geophysical, hydrochemical, and hydrologic data sets with numerical modeling to resolve recharge mechanisms for freshwater emplacement on New England's Continental Shelf and better understand the

origin of overpressure beneath Nantucket. The utilization of geophysical data is a cost-effective method to obtain spatial information regarding the salinity concentrations beneath Nantucket Island that could not be obtained easily by drilling. It provided valuable, qualitative insight for construction of numerical groundwater models; moreover, the geophysical data were used to help evaluate models that might explain the observed modern hydrologic conditions on Nantucket. This work points toward future, fully integrated analyses, in which geophysical data might provide quantitative information for model calibration through regression methods. Integrating the hydrochemical and hydrological data sets with the numerical modeling allowed us to investigate the relationship between hydromechanical loading of the Laurentide Ice Sheet and sediment loading associated with the high sedimentation rate of the Late Pleistocene and the hydrologic response of the resulting from variable sea level changes and increased recharge from the last glacial maximum.

The TDEM soundings indicate a freshwater/saltwater transition or interface at about 120 mbsl on Nantucket, whereas the solute diffusion profile from USGS 6001 and our numerical modeling indicate a deeper interface. This apparent inconsistency can be explained by either (1) the presence of trapped, saline water in confining units, and/or (2) confining units that include substantial low-resistivity clay. The approximate maximum depth of investigation for the TDEM surveys is about 120 m; thus any deeper transitions back to freshwater would not be detected by these geophysical data. The presence of low-resistivity confining units would also explain sounding results from TDEM sites 14 and 15, where the resistivity was too high for saltwater-saturated sands but too low for freshwater-saturated.

Results of the numerical modeling indicate that the high hydraulic heads associated with the Laurentide Ice Sheet and Glacial Lake Nantucket substantially influenced the distribution of freshwater beneath Nantucket and the fluid pressure distribution across the Continental Shelf. Although sea level varied substantially during the Pleistocene, hydraulic heads experienced during sea level low stands would not have been high enough to flush salty waters from the deep Cretaceous and Tertiary aquifers below Nantucket. Both TDEM soundings and mathematical model results suggest the transition from fresh to saltwater within confined aquifers of the Atlantic Continental Shelf occurs near the southern terminus of Nantucket Island.

Both the loading associated with the Laurentide Ice Sheet and the high sedimentation rates associated with the Late Pleistocene had profound effects on the hydraulic heads on the Continental Shelf. We believe that we have found, perhaps for the first time, evidence of "fossil pressures" from Late Pleistocene glaciation. Large amounts of freshwater were emplaced during the glacial maximum when extremely high hydraulic heads were present on the Continental Shelf. Long response times of low-permeability clays facilitate the retention of high pressures induced during the glacial maximum. As the ice sheet retreats and sedimentation rates increase on the shelf, fluid pressures continue to increase. After sedimentation rates decrease, high pressures generated in these deep clays could have easily been laterally transferred toward shallower sediment near the coastline. The high heads observed in well USGS 6001 may be the first recorded observations of fossil heads from the last glacial maximum. Previous evidence for sub-ice-sheet recharge comes entirely from geochemical and environmental isotopic

data [Boulton et al., 1995; Piotrowski, 1997; Siegel and Mandle, 1984; and Grasby et al., 2000].

The results of this study have important implications for all New England coastal aquifers in that (1) freshwater resources cannot be inferred by modern sea level conditions, and (2) glacial recharge and high sedimentation rates in the Late Pleistocene may substantially control the modern spatial distribution of freshwater. We found that Late Pleistocene recharge rates were at least 10 times greater than present day conditions. This phenomenon may also account for unusually freshwater observed at significant depths offshore New Jersey and New York [Hathaway et al., 1979; Kohout et al., 1988] as well as the high fluid pressures observed on the continental slope [Dugan and Flemings, 2000].

References

Bear, J., *Dynamics of Fluids in Porous Media*, Dover Publications, New York, pp. 784, 1972.

Bekele, E. B., B. J. Rostron, and M. A. Person, Fluid pressure implications of erosional unloading, basin hydrodynamics and glaciation in the Alberta Basin, Western Canada, *Journal of Geochemical Exploration*, *78-79*, 143-147, 2003.

Bense, V. F., and M. A. Person, Faults as conduit-barrier systems to fluid flow in siliciclastic sedimentary aquifers, *Water Resources Research*, *42(5)*, W05421, 2006.

Bethke, C. M., and T. F. Corbet, Linear and nonlinear solutions for one-dimensional compaction flow in sedimentary basins, *Water Resources Research, 24(3)*, 461-467, 1988.

Boulton, G. S., P. E. Caban, and K. van Gijssel, Groundwater flow beneath ice sheets: Part I - Large scale patterns, *Quaternary Science Reviews, 14(6),* 545-562, 1995.

Boulton, G. S., and P. Caban, Groundwater flow beneath ice sheets: Part II - Its impact on glacier tectonic structures and moraine formation, *Quaternary Science Reviews, 14(6)*, 563-587, 1995.

Clark, P. U., Unstable behavior of the Laurentide ice sheet over deforming sediment and its implications for climate change, *Quaternary Research, 41(1),* 19-25, 1994.

Corbet, T. F., and C. M. Bethke, Disequilibrium fluid pressures and groundwater flow in the western Canada sedimentary basin, *Journal of Geophysical Research, 97(B5)*, 7203-7217, 1992.

Denton, G. H., and T. J. Hughes, *The Last Great Ice Sheets*, John Wiley and Sons, New York, pp. 484, 1981.

Drabbe, J., and W. Badon-Ghyben, Nota in verband met de voorgenomen putboring nabij Amsterdam, in *Tijdschrift van het Koninklijk Institut van Ingenieurs*, Netherlands, The Hague, 1889.

Dugan, B., and P. B. Flemings, Overpressure and fluid flow in the New Jersey continental slope: Implications for slope failure and cold seeps, *Science, 289(5477)*, 288-291, 2000.

Fitterman, D. V., and M. Deszcz-Pan, Geophysical mapping of saltwater intrusion in Everglades National Park, *U. S. Geological Survey Open-File Report, 99-0181*, 16-17, 1999.

Fitterman, D. V., and M. T. Stewart, Transient electromagnetic sounding for groundwater, *Geophysics, 51(4)*, 995-1005, 1986.

Folger, D. W., J. C. Hathaway, R. A. Christopher, P. C. Valentine, and C. W. Poag, Stratigraphic test well, Nantucket Island, Massachusetts, *U. S. Geological Survey Circular, C 773*, 28, 1978.

Freeze, R. A., and J. A. Cherry, *Groundwater*, Prentice-Hall, New Jersey, pp. 604, 1979.

Garven, G., A hydrogeologic model for the formation of the giant oil sands deposits of the western Canada sedimentary basin, *American Journal of Science, 289(2)*, 105-166, 1989.

Giles, M. R., *Diagenesis: A Quantitative Perspective*, Kluwer Academic Publishers, Boston, Massachusetts, pp. 526, 1997.

Grasby, S., K. Osadetz, R. Betcher, and F. Render, Reversal of the regional-scale flow system of the Williston basin in response to Pleistocene glaciation, *Geology, 28(7)*, 635-638, 2000.

Groen, K., The effects of transgressions and regressions on coastal and offshore groundwater, Ph. D. Thesis Vrije Universiteit Amsterdam, 2002.

Gutierrez, B. T., E. Uchupi, N. W. Driscoll, and D. G. Aubrey, Relative sea-level rise and the development of valley-fill and shallow-water sequences in Nantucket Sound, Massachusetts, *Marine Geology, 193(3-4)*, 295-314, 2003.

Hall R. E., L. J. Poppe, and W. M. Ferrebee, A stratigraphic test well, Martha's Vineyard, Massachusetts, *U. S. Geological Survey Bulletin, B 1488,* 1980.

Haq, B. U., J. Hardenbol, and P. R. Vail, Chronology of fluctuating sea levels since the Triassic, *Science, 235(4793)*, 1156-1167, 1987.

Hathaway, J. C., C. W. Poag, P. C. Valentine, R. E. Miller, D. M. Schultz, F. T. Manheim, F. A. Kohout, M. H. Bothner, and D. A. Sangrey, U. S. Geological Survey core drilling on the Atlantic shelf, *Science, 206(4418),* 515-527, 1979.

Hays, J. D., J. Imbrie, and N. J. Shackleton, Variations in the Earth's orbit: Pacemaker of the ice ages, *Science, 194 (4270)*, 1121-1132, 1976.

Herzberg, A., Die Wasserversorgung einiger Nordseebäder, *Journal für Gasbeleuchtung und Wasserversorgung, 44*, 815–819, 842-844, 1901.

Hubbert, M. K., and W. W. Rubey, Role of fluid pressure in mechanics of overthrust faulting I. Mechanics of fluid-filled porous solids and its application to overthrust faulting, *Geological Society of America Bulletin, 70(2)*, 115-166, 1959.

Imbrie, J., A theoretical framework for the Pleistocene ice ages, *Journal of the Geological Society of London, 142(3)*, 417-432, 1985.

Kestin, J., H. E. Khalifa , and R. Corriea, Tables of the dynamics and kinematic viscosity of aqueous NaCl solutions in the temperature range of 20-150° C and the pressure range of 0.1-35 MPa, *Journal of Physical Chemistry Reference Data, 10*, 71-87, 1981.

Kohout, F. A., J. C. Hathaway, D. W. Folger, M. H. Bothner, E. H. Walker, D. F. Delaney, M. H. Frimpter, E. G. A. Weed, and E. C. Rhodehamel, Fresh ground water stored in aquifers under the continental shelf: implications from a deep test, Nantucket Island, Massachusetts, *Water Resources Bulletin, 13(2)*, 373-386, 1977.

Kohout, F. A., H. Meisler, F. W. Meyer, R. H. Johnston, G. W. Leve, and R. L. Wait, Hydrogeology of the Atlantic continental margin, in *The Atlantic Continental Margin: U. S.*, edited by R. E. Sheridan and J. A. Grow, The Geological Society of America, Boulder, CO, 463-480, 1988.

Kooi, H., and J. Groen, Offshore continuation of coastal groundwater systems; predictions using sharp-interface approximations and variable-density flow modelling, *Journal of Hydrology, 246(1-4)*, 19-35, 2001.

Kooi, H., J. Groen, and A. Leijnse, Modes of seawater intrusion during transgressions, *Water Resources Research, 36(12)*, 3581-3589, 2000.

Lemieux, J. M., E. A. Sudicky, W. R. Peltier, and L. Tarasov, Coupling glaciations with groundwater flow models – Surface/subsurface interactions over the Canadian landscape during the Wisconsinan glaciation, IAHR – GW 2006, International Groundwater Symposium, Toulouse, June 12-14, 2006.

Lerche, I., Z. Yu, B. Tørudbakken, and R. O. Thomsen, Ice loading effects in sedimentary basins with reference to the Barents Sea, *Marine and Petroleum Geology, 14(3)*, 277-338, 1997.

Lucia, F. J., Rock-fabric/petrophysical classification of carbonate pore space for reservoir characterization, *American Association of Petroleum Geologists Bulletin, 79(9),* 1275-1300, 1995.

Marquardt, D. W., An algorithm for least-squares estimation of nonlinear parameters, *Journal of the Society for Industrial and Applied Mathematics, 11*, 431-441, 1963.

Masterson, J. P., B. D. Stone, D. A. Walters, and J. Savoie, Hydrogeologic framework of western Cape Cod, Massachusetts, *Hydrologic Investigations Atlas, HA*-741, 1997.

McWhorter, D. B., and D. K. Sunada, *Groundwater Hydrology and Hydraulics*, Water Resources Publications, Highland Ranch, Colorado, pp. 287, 1977.

Meisler, H., P. P. Leahy, and L. L. Knobel, Effect of eustatic sea-level changes on saltwater-freshwater relations in the northern Atlantic coastal plain, *U. S. Geological Survey Water-Supply Paper, 2255*, 1984.

Mills, T., P. Hoekstra, M. Blohm, and L. Evans, Time domain electromagnetic soundings for mapping sea-water intrusion in Monterey County, California, *Ground Water, 26(6)*, 771-782, 1988.

Nabighian, M. N., and J. C. Macnae, Time domain electromagnetic prospecting methods, in *Electromagnetic Methods in Applied Geophysics Volume 2, Application, Part A*, edited by M. N. Nabighian, Society of Exploration Geophysicists, Tulsa, OK, 427-520, 1991.

Neuzil, C. E., How permeable are clays and shales?, *Water Resources Research, 30(2)*, 145-150, 1994.

O'Hara, C. J., and R. N. Oldale, Maps showing geology, shallow structure and bedform morphology of Nantucket Sound, Massachusetts, *U. S. Geological Survey Miscellaneous Fields Studies Map, MF-1911,* 1987.

Oldale, R. N., Geologic map of Nantucket and nearby islands, Massachusetts, *U. S. Geological Survey Miscellaneous Investigations Series, I-1580, 1985.*

Oldale, R. N., and C. J. O'Hara, New radiocarbon dates from the inner continental shelf off southeastern Massachusetts and a local sea-level-rise curve for the past 12,000 yr, *Geology, 8(2)*, 102-106, 1980.

Oldale, R. N., and C. J. O'Hara, Glaciotectonic origin of the Massachusetts coastal end moraines and a fluctuating late Wisconsinan ice margin, *Geological Society of America Bulletin, 95*, 61-74, 1984.

Peltier, W. R., Postglacial variations in the level of the sea: Implications for climate dynamics and solid-Earth geophysics, *Reviews of Geophysics, 36(4)*, 603-689, 1998.

Person, M., B. Dugan, J. B. Swenson, L. Urbano, C. Stott, J. Taylor, and M. Willett, Pleistocene hydrogeology of the Atlantic continental shelf, New England, *Geological Society of America Bulletin, 115(11)*, 1324-1343, 2003.

Person, M., J. McIntosh, V. Bense, and V. H. Remenda, Pleistocene hydrology of north America: The role of ice sheets in reorganizing groundwater flow systems, *Reviews of Geophysics*, in press, 2007.

Person, M., J. Z. Taylor, and S. L. Dingman, Sharp interface models of salt water intrusion and wellhead delineation on Nantucket Island, Massachusetts, *Ground Water, 36(5)*, 731-742, 1998.

Piotrowski, J. A., Subglacial hydrology in north-western Germany during the last glaciation: Groundwater flow, tunnel valleys and hydrological cycles, *Quaternary Science Reviews, 16(2)*, 169-185, 1997.

Raymo, M. E., W. F. Ruddiman, J. Backman, B. M. Clement, and D. G. Martinson, Late Pliocene variation in northern hemisphere ice sheets and north Atlantic deep water circulation, *Paleoceanography, 4(4)*, 413-446, 1989.

Raymo, M. E., D. W. Oppo, and W. Curry, The mid-Pleistocene climate transition: a deep sea carbon isotopic perspective, *Paleoceanography, 12(4*), 546-559, 1997.

Redfield, A. C., and M. Rubin, The age of salt marsh peat and its relation to recent changes in sea level at Barnstable, Massachusetts, *Proceedings of the National Academy of Sciences of the United States of America, 48 (10)*, 1728-1735, 1962.

Schlee, J. S., and J. Fritsch, Seismic stratigraphy of the Georges Bank Basin complex, offshore New England, *American Association of Petroleum Geologists Memoir, 34*, 223-251, 1982.

Scholle, P. A., Geological studies of the COST No. B-2 well, U. S. mid-Atlantic outer continental slope area, *Geological Survey Circular, C-750*, 1977.

Scholle, P. A., Geological studies of the COST No. B-3 Well, United States mid-Atlantic continental slope area, *Geological Survey Circular, C-833*, 1980.

Shackleton, N. J., and N. D. Opdyke, Oxygen isotope and palaeomagnetic stratigraphy of equatorial Pacific core V28-238: Oxygen isotope temperatures and ice volumes on a 10^5 year and 10^6 year scale, *Quaternary Research, 3(1)*, 39-55, 1973.

Shackleton, N. J., Oxygen isotopes, ice volume, and sea level, *Quaternary Science Reviews, 6 (3-4)*, 183-190, 1987.

Shenhav, H., Lower Cretaceous sandstone reservoirs, Israel; Petrography, porosity, permeability, *American Association of Petroleum Geologists Bulletin, 55(12)*, 2194-2224, 1971.

Shreve, R. L., Late Wisconsin ice-surface profile calculated from esker paths and types, Katahdin esker system, Maine, *Quaternary Research, 23(1)*, 27-37,1985.

Siegel, D. I., and R. J. Mandle, Isotopic evidence for glacial meltwater recharge to the Cambrian-Ordovician aquifer, north-central United States, *Quaternary Research, 22(3)*, 328-335, 1984.

Summerhayes, C. P., Sealevel curves based on seismic stratigraphy: Their chronostratigraphic significance, *Palaeogeography, Palaeoclimatology, Palaeoecology, 57(1)*, 27-42, 1986.

Taylor, D., and R. C. Anderson., Geophysical studies of the COST nos. G-1 and G-2 wells, United States north Atlantic outer continental shelf, *Geological Survey Circular, C-861*, 1982.

Uchupi, E., N. Driscoll, R. D. Ballard, and S. T. Bolmer, Drainage of late Wisconsin glacial lakes and the morphology and late Quaternary stratigraphy of the New Jersey – southern New England continental shelf and slope, *Marine Geology, 172(1-2)*, 117-145, 2001.

Vail, P. R., and J. Hardenbol, Sea-level changes during the Tertiary, *Oceanus, 22(3)*, 71-79, 1979.

van der Veen, C. J., *Fundamentals of Glacier Dynamics*, A. A. Balkema, Rotterdam, The Netherlands, pp. 472, 1999.

Zheng, C., and G. D. Bennett, *Applied Contaminant Transport Modeling*, Van Nostrand Reinhold, New York, pp. 621, 1995.

VITAE

ANDEE J. MARKSAMER

E-mail: amarksamer@gmail.com

Date of Birth: March 26, 1979
Place of Birth: Bethpage, NY

Education

Master of Science, Geological Sciences - Indiana University, Bloomington, IN
May 2007
Thesis: Integrating Geophysical, Hydrochemical, and Hydrologic Data to Understand the Freshwater Resources on Nantucket Island, Massachusetts
Advisor: Dr. Mark Person

Bachelor of Arts, Earth and Environmental Science -Wesleyan University, Middletown, CT
May 2001

Employment/Fellowships

Chevron Summer Intern - Chevron Corporation, Houston, TX
Summer 2006
Worked within G&G Operations in Deep Water Gulf of Mexico. Performed pore pressure and wellbore stability analysis for wells within the deep water Gulf of Mexico business unit. Assisted in building a work flow for generating 3D pore pressure cubes in Gocad.

Chevron Texaco Fellowship – Indiana University, Bloomington, IN
Fall 2005
Awarded the Chevron Texaco Fellowship for the fall semester of 2005 by the Indiana University Department of Geological Sciences.

Research Assistant- Indiana University, Bloomington, IN
Summer 2004-Summer 2005, Spring 2006, Fall 2006
Worked 20 hours a week conducting research for Dr. Mark Person within his GeoFluids Computational Laboratory. Research included building 2D and 3D meshes of geologic units, revising fortran code used in finite element groundwater modeling and running groundwater models, analyzing groundwater samples for $\delta^{18}O$ and δD, determining mineralogy of clay samples using x-ray diffraction, conducting radial diffusion experiments and porosity measurements.

Staff Scientist I/Staff Scientist II- LFR Levine Fricke Inc., East Hartford, CT
August 2001-July 2004

Conducted Phase I, Phase II, and Phase III Environmental Site Assessments (ESA) for residential, commercial, and industrial properties; developed recommendation letters and budget proposals regarding further work for ESAs; directed drilling and construction contractors at sites for Phase II and III ESAs; performed groundwater sampling. Promoted to Staff Scientist II in March 2003.

Undergraduate Researcher - United States Geological Survey, Woods Hole, MA
Summer 1999
Worked on a Seafloor GIS Mapping Project entering data in a GIS program, worked on a week long seafloor mapping research cruise recording data and video of the seafloor; participated on a ten day research cruise studying the effects of fishing on seafloor biodiversity, sorting benthic organisms pulled up in a dredge.

Hughes Fellowship - Wesleyan University, Middletown, CT
Summer 1998
Worked in a sedimentology lab studying past climate change through size analysis of seafloor sediment using sieving techniques and a sedigraph. Created a poster describing the project and presented it at an all-campus poster presentation.

Publications

Marksamer, Andee J., M. Person, F. Day-Lewis, J. W. Lane, D. Cohen, B. Dugan ,K. Henk, and M. Willett. Integrating Geophysical, Hydrochemical, and Hydrologic Data to Understand the Freshwater Resources on Nantucket Island, Massachusetts. In Hyndman, D.W., F. D. Day-Lewis, and K. Singha (eds.) *Data Integration in Subsurface Hydrology*, AGU Water Resources Monograph, *in press* 2007.

Meetings and Short Courses

Geological Society of America - Fall 2005 Meeting, Salt Lake City, UT
October 2005
Presented a poster entitled Hydrogeology of a Glacio-Lacustrine Sediment on Nantucket, MA.

Sequence Stratigraphy for Graduate Students Short Course -*Salt Lake City, UT*
Geological Society of America Fall 2005 Meeting - October 2005
Course was Co-sponsored by ExxonMobil and British Petroleum

Certifications

OSHA 40 Hour HAZWOPER August 2001
OSHA 8 Hour HAZWOPER refresher March 2003
Hazardous Materials Transportation Certification (49 CFR Parts 100-185) Nov. 2002
SafeGulf- Chevron Corporation, Summer 2006